forests

MDPI

Article

Discovery and Profiling of microRNAs at the Critical Period of Sex Differentiation in *Xanthoceras sorbifolium* Bunge

Xu Wang, Yaqi Zheng, Shuchai Su and Yan Ao *

Key Laboratory for Silviculture and Conservation, Ministry of Education, Beijing Forestry University, Beijing 100083, China; wx19941019@sina.com (X.W.); yaaqiqiqi@163.com (Y.Z.); sushuchai@sohu.com (S.S.)
* Correspondence: aoyan@bjfu.edu.cn

Received: 21 October 2019; Accepted: 11 December 2019; Published: 13 December 2019

Abstract: Research Highlights: The critical period of sex differentiation in *Xanthoceras sorbifolium* was investigated. Multiple microRNAs (miRNAs) were identified to influence female and male flower development, with some complementary functions. Background and Objectives: *Xanthoceras sorbifolium* Bunge is widely cultivated owing to its multipurpose usefulness. However, as a monoecious plant, the low female–male flowers ratio and consequent low seed yield are the main bottlenecks for industrial-scale development of seed utilization. MiRNAs play crucial regulatory roles in flower development and sex differentiation; therefore, we evaluated the roles of miRNAs in the critical period of sex differentiation in *X. sorbifolium*. Materials and Methods: Four small RNA libraries for female and male flower buds of the critical period of sex differentiation were constructed from paraffin-embedded sections. The miRNAs were characterized by high-throughput sequencing, and differentially expressed miRNAs were validated by reverse transcription-quantitative polymerase chain reaction. Results: There were obvious differences in male and female pistil and stamen flower buds, with elongated inflorescence and clear separation of flower buds marking the critical period of sex differentiation. A total of 1619 conserved miRNAs (belonging to 34 families) and 219 novel miRNAs were identified. Among these, 162 conserved and 14 novel miRNAs exhibited significant differential expression in the four libraries, and 1677 putative target genes of 112 differentially expressed miRNAs were predicted. These target genes were involved in diverse developmental and metabolic processes, including 17 miRNAs directly associated with flower and gametophyte development, mainly associated with carbohydrate metabolism and glycan biosynthesis and metabolism pathways. Some miRNA functions were confirmed, and others were found to be complemented. Conclusions: Multiple miRNAs closely related to sex differentiation in *X. sorbifolium* were identified. The theoretical framework presented herein might guide sex ratio regulation to enhance seed yield.

Keywords: *Xanthoceras sorbifolium* Bunge; microRNAs; sex differentiation; high-throughput sequencing; RT-qPCR

1. Introduction

Xanthoceras sorbifolium Bunge is a perennial small tree or shrub belonging to the Sapindaceae family [1]. The plant fruits in the third year after sowing, and has a lifespan of more than 200 years with high resistance to drought, barren, saline, and alkaline soil, and can survive extreme temperatures between −30 °C and −41 °C [2–5]. *X. sorbifolium* has been cultivated for thousands of years in northern China for its smokeless illuminating oil, cooking oil, and as traditional medicine [6]. *X. sorbifolium* is also widely recognized for its ecological and landscaping value [7]. There has been increased interest in this species in recent years owing to its high seed kernel oil concentration (55–66%), proving to be

a valuable feedstock for biodiesel production [8–11]. The seed oil is rich in unsaturated fatty acids (>93%), mainly linoleic and oleic acids [1], which play an essential role in biodiesel quality. Accordingly, researchers have attempted to explore its broad traits as feedstock for biodiesel and to utilize its valuable byproducts. Furthermore, the seed cake is characterized by high protein content and can be used as fertilizer, plant protein beverage, or animal feed, and the saponins and sterol in the seed cake and fruit peel have high medicinal value. This immense economic potential and environmental significance of *X. sorbifolium* as a replacement for fossil fuels has materialized in large-scale plantations, with at least 1.33×10^5 ha of *X. sorbifolium* cultivated from 2006 to 2010, and the total area is expected to exceed 5×10^5 ha in 2020 [1].

To best exploit *X. sorbifolium*'s features for economic profit and ecological benefit, it is essential to select and breed germplasm resources with high seed production. From a botanical perspective, seed production mainly depends on flower production and fruit setting. *X. sorbifolium* is a monoecious plant, and the low abundance of female flowers and the ratio of female to male flowers are currently considered the primary factors limiting seed yield. *X. sorbifolium* produces flowers on a racemose inflorescence. The female flowers usually occur in apical inflorescences, whereas male flowers mostly flourish in lateral inflorescences, resulting in a highly biased male flower ratio [12,13]. Typically, both flowers are initially bisexual, with female and male organs showing identical formation patterns. However, when reaching the critical period of sex differentiation, the stamens of male flowers develop normally, while the pistil enters a state of selective arrest [14]. By contrast, in female flowers, the anthers do not dehisce due to abortion of the stamens, with no further differentiation and development, whereas the ovary continues to develop and can bear fruits [15–18] (Figure 1). Therefore, for *X. sorbifolium*, male flowers dominate over the female flowers. Enhancing the number of female flowers would be an effective way to improve the output and obtain large-scale benefits from the seed. The selective developmental arrest of preformed organ primordia is currently the most common method for generating unisexual flowers [19]. However, a deeper understanding of the molecular mechanisms contributing to sex differentiation would provide new strategies for breeding to enhance the number of female flowers and improve yield.

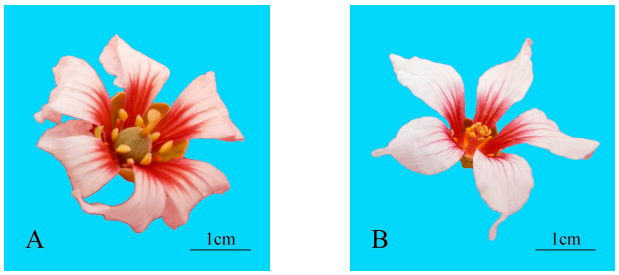

Figure 1. Flowers of *Xanthoceras sorbifolium;* (**A**) female flowers; (**B**) male flowers.

MicroRNAs (miRNAs) are a class of endogenous non-coding sRNAs with a size of 21–24 nucleotides (nt) that widely exist in eukaryotes [20,21]. As a negative regulator of gene expression, miRNAs play critical roles in the transcriptional and post-transcriptional regulation of many genes related to plant growth and developmental processes, such as organ morphogenesis, phase change, fruit development, defense against stress, hormone synthesis, and signal transduction [22–26]. In addition, some miRNAs have been identified to play a role in sex determination in plants. For example, miR159 controls the development of anthers by regulating the expression of its target genes *MYB33* and *MYB65* [27,28]. In addition, miR319 affects ethylene and auxin synthesis through regulating the expression of the auxin-related factor *ARF2*, while miR156 and miR172 play opposite roles in controlling flowering time by targeting *SPL* and *AP2*, respectively [29–31]. Moreover, Banks found that miR172e, encoded by the *ts4* gene, acts on an *APETALA2* homologous transcription factor (*ids1*) to inhibit pistil development in male flowers of monoecious maize [32]. Recent studies have also

suggested that miRNAs are differentially expressed during the sex determination period and have been found to play specific regulatory roles in model plants [33]. Therefore, regulating the expression of miRNAs can be a new strategy to improve the sex ratio of monoecious plants, including *X. sorbifolium*.

Although the effects of miRNA on sex regulation have been reported for many plant species, including *Arabidopsis* and maize [27,28,32], the biological information of miRNAs of *X. sorbifolium* remains limited, and this research is in the initial stage. These studies have mainly focused on flower organ mutants [34–36], and there has been no comprehensive study of the miRNA expression profiles in *X. sorbifolium* performed to date. Therefore, this study aimed to identify the miRNAs involved in the formation of female and male flowers during the critical period of sex differentiation in *X. sorbifolium*. High-throughput sequencing was used to sequence small RNA (sRNA) libraries of female and male flowers in the critical period of sex differentiation. Conserved and novel miRNAs and their target genes were identified and predicted using bioinformatics tools, and miRNAs expression levels were compared between the two kinds of flowers in different periods to identify differentially expressed miRNAs. Reverse transcription-quantitative polymerase chain reaction (RT-qPCR) was then employed to validate the expression levels of selected miRNAs in male and female flowers. These results can provide a basis for increasing the ratio of female to male flowers to enhance yield, along with a general insight into the mechanisms underlying sex determination in monoecious plants.

2. Materials and Methods

2.1. Plant Materials

Female and male flower buds of 10-year-old *X. sorbifolium* were collected from a mature plantation in Dongying city, Shandong province, China, from when inflorescences started to elongate (27 March 2018) (Figure 2A1,A2) to when they began to flower (13 April 2018) (Figure 2F1,F2) with four periodic intervals in between (31 March, 3 April, 7 April, and 10 April) (Figure 2). Five well-grown individuals were randomly sampled. From each of the five trees, 10 flower buds at the middle part of apical inflorescences (female) were mixed as a biological sample and subjected to three biological replicates; the same was true of buds at lateral inflorescences (male) [12]. The samples were divided into two parts: one was immediately frozen in liquid nitrogen and stored at −80 °C for further use, and the other was fixed in formalin/acetic acid/70% ethanol (FAA) at a ratio of 5:5:90 for paraffin sectioning [7].

Figure 2. Inflorescence development process of male and female flowers in *X. sorbifolium*. (**A1**), (**B1**), (**C1**), (**D1**), (**E1**), and (**F1**): Inflorescences of a female flower on 27 March, 31 March, 3 April, 7 April, 10 April, and 13 April, respectively; (**A2**), (**B2**), (**C2**), (**D2**), (**E2**), and (**F2**): Inflorescences of a male flower on 27 March, 31 March, 3 April, 7 April, 10 April, and 13 April, respectively.

2.2. Critical Period Determination

Paraffin sections were microscopically examined to determine the critical period of sex differentiation. The FAA-embedded samples were dehydrated using an ethanol series (50–100%),

infiltrated with toluene and paraffin, and supplemented with paraffin (24 h, 36–60 °C). After solidification of the paraffin, the samples were cut into 10-µm-thick sections, which were stained with safranin O and fast green, and observed and photographed using an Olympus CX-41 optical microscope (Olympus, Tokyo, Japan).

2.3. RNA Extraction, Libraries Construction, and High-Throughput Sequencing

Total RNA was isolated with Quick RNA Isolation Kit (Huayueyang, Beijing, China) according to the manufacturer's protocol using three biological replicates. The total RNA quality was tested using 1% agarose gel electrophoresis and a NanoDrop ND-1000 spectrophotometer (Thermo Fisher Scientific, Waltham, MA, USA). For each replication, four sRNA libraries (female and male flower buds of the two phases, respectively) were constructed and sequenced on the Illumina HiSeq platform at Beijing Yuanquanyike Biological Technology Co., Ltd. (Beijing, China). Briefly, the 3′ SR (3′ single read) adapter was ligated to the 3′ end of RNA, and the RT primer was hybridized to the 3′ SR adapter to transform the single-stranded DNA adaptor into a double-stranded DNA molecule. The 5′ SR (5′ single read) adapter was then ligated to the 5′ end of RNA, followed by reverse transcription with reverse transcriptase. The initial libraries were then amplified using PCR to generate stable libraries for sequencing. The final stable libraries contained adapter sequences for sequencing and index sequences to distinguish different samples. Finally, polyacrylamide gel electrophoresis was used to recover libraries containing only sRNAs with a size of about 150 bp.

2.4. Bioinformatics Analysis

After sequencing, raw sequence reads of the four libraries were cleaned of adapter sequences, low-quality tags, reads containing polyA or polyT, and reads smaller than 15 or larger than 34 nt using cutadapt [37]. The clean reads in the range of 15–34 nt were then aligned to Rfam [38] to filter rRNAs, tRNAs, snRNA, and sRNAs other than miRNAs. The remaining sequences were assembled into unique sRNAs, which were analyzed via a BLAST search against miRBase [39], allowing a maximum of one mismatch to identify conserved miRNAs. The unique sRNAs that did not map to known miRNAs or the other kinds of sRNAs were mapped to the reference genome [40] using bowtie2 [41]. MIREAP was used to predict novel miRNAs based on the mapping result [42].

miRNAs from the four libraries were subjected to four kinds of comparisons: two comparisons between female and male flower buds at the same phase (Fa vs. Ma and Fb vs. Mb), and two comparisons between the two phases of the same sex bud (Fa vs. Fb and Ma vs. Mb). For each miRNA group, the read count was normalized to the RPM (reads per million) value. Fold change and p-values were used to identify differentially expressed miRNAs in each comparison: if $\log_2$ (fold change) > 1 or $\log_2$ (fold change) < -1 and $p < 0.05$, the miRNA was considered to be significantly differentially expressed between libraries. The potential target genes of differentially expressed miRNAs were predicted according to the intersection of miRanda [43] and RNAhybrid predictions [44]. Gene Ontology (GO) [45] and Kyoto Encyclopedia of Genes and Genomes (KEGG) [46] were used to annotate potential target gene functions.

2.5. Validation of Differentially Expressed miRNAs with RT-qPCR

To validate the expression of miRNAs obtained from high-throughput sequencing, 16 of the conserved miRNAs and three novel miRNAs with differential expression were subjected to RT-qPCR. Total RNA was respectively extracted from different sex buds of the two phases and converted to cDNA with TransScript® miRNA First-Strand cDNA Synthesis Super Mix (Transgen Biotech, Beijing, China). qPCR was performed on a Step One Plus machine (Applied Biosystems, Foster City, CA, USA) in three biological replicas. The forward primers of these 19 miRNAs were specifically designed according to the miRNA sequences, and the universal primer was used as the reverse primer. The U6 snRNA was used as a reference gene for normalization. All the primers used for RT-qPCR are shown in Table S1. Each 10-µL reaction mix contained 2 µL cDNA, 5 µL TB Green Premix Ex Taq II, 0.2 µL Rox

Reference Dye, 2.3 µL RNase-free water, and 0.25 µL each primer, which was prepared using an SYBR® Premix Ex Taq II kit (Takara, Beijing, China). The conditions for PCR amplification were as follows: pre-denaturation at 95 °C for 3 min, followed by 40 cycles of 95 °C for 30 s, 60 °C for 30 s, and 72 °C for 30 s. The relative gene expression level was calculated using the comparative Ct method ($2^{-\Delta\Delta CT}$) [47].

3. Results

3.1. Determination of the Critical Period of Sex Differentiation

To determine the critical period of sex differentiation, we first identified the time at which the pistil and stamen begin to abort (Figure 3). Microscopic observations of paraffin-embedded sections showed no obvious structural difference between male and female flower pistils in the initial periods (Figure 3A1–C2). However, an obvious difference in pistils appeared on 7 April (Figure 3D1,D2). The female flower was characterized by a well-developed globose ovary, with carpels separating the plump ovules, papillary cells evident on the stigma, and the pistil grew towards maturation (Figure 3D1). Conversely, the ovary and ovule of the male flower showed a tendency to shrink and arrest, only rudimentary ovules were formed, and there was no papillary cell on the stigma (Figure 3D2). Simultaneously, the external morphology of male and female inflorescences differed at this stage compared to that observed in the previous periods. The flower buds grew faster and began to separate from each other; the transverse and vertical diameters of female flower buds were 2.53–3.90 mm and 2.62–4.14 mm, whereas those of males were 2.66–4.15 mm and 2.76–4.34 mm, respectively (Figure 2D1,D2). As development progressed, the pistil of the female flower elongated and expanded, the papillary cells became denser and larger (Figure 3E1,F1), and the stigma grew towards development and maturation. By contrast, there was no further differentiation and development in the pistil of the male flower, and the female tissues eventually underwent abortion (Figure 3E2,F2).

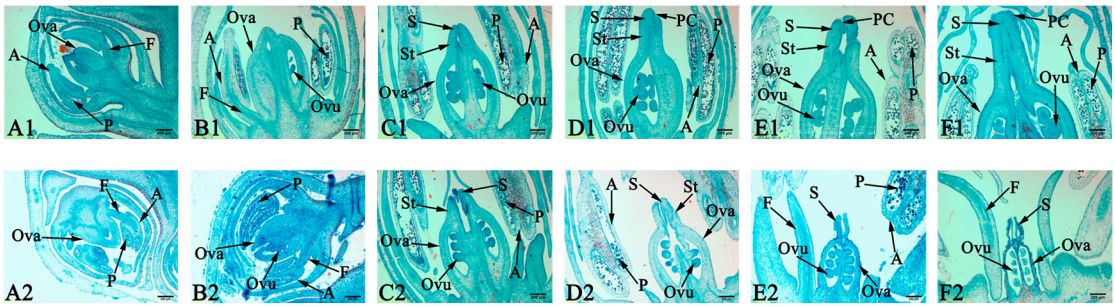

Figure 3. Pistil development process of male and female flowers in *X. sorbifolium*. (**A1**), (**B1**), (**C1**), (**D1**), (**E1**), and (**F1**): Pistil morphology of a female flower on 27 March, 31 March, 3 April, 7 April, 10 April, and 13 April, respectively; (**A2**), (**B2**), (**C2**), (**D2**), (**E2**), and (**F2**): Pistil morphology of a male flower on 27 March, 31 March, 3 April, 7 April, 10 April, and 13 April, respectively; Ova—Ovary; Ovu—Ovule; St—Style; S—Stigma; F—Filament; A—Anther; P—Pollen; PC—Papillary cell.

Clear differences were also detected in the stamens of the two types of flowers on 7 April. The stamen of the female flower ceased elongation, while that of the male flower continued to grow to maturity (Figure 3D1,D2). The internal structure of the pollens also began to show distinct sex differentiation on 7 April (Figure 4). The pollens of the female flower were vacuolated with no visible nuclei of the pollen grains, and the cytoplasm was thin (Figure 4D1). However, in the male flower, the pollen grew into a round shape containing well-developed nuclei, and the pollen grains were thick (Figure 4D2). During subsequent development, the pollens of the female flower were further vacuolated and eventually lost their male function (Figure 4F1), while those of the male flowers normally developed and were functional (Figure 4F2) [48].

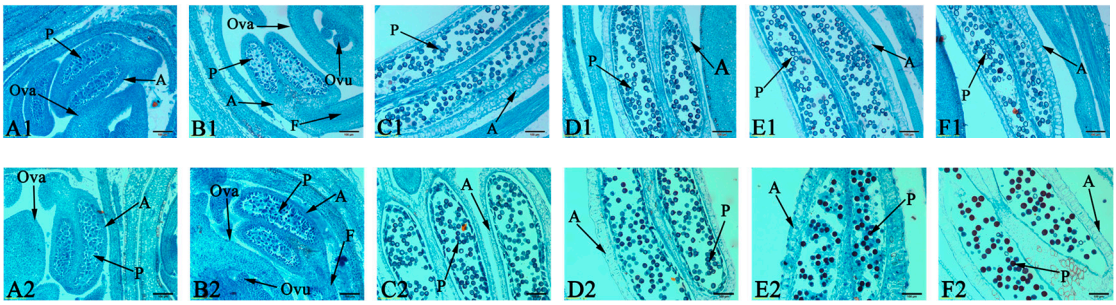

Figure 4. Stamens development in male and female flowers of *X. sorbifolium*. (**A1**), (**B1**), (**C1**), (**D1**), (**E1**), and (**F1**): Pollen morphology of a female flower on 27 March, 31 March, 3 April, 7 April, 10 April, and 13 April, respectively; (**A2**), (**B2**), (**C2**), (**D2**), (**E2**), and (**F2**): Pollen morphology of a male flower on 27 March, 31 March, 3 April, 7 April, 10 April, and 13 April, respectively; Ova—Ovary; Ovu—Ovule; F—Filament; A—Anther; P—Pollen.

Based on these results, the period from 31 March to 7 April was regarded as the critical period of sex differentiation of *X. sorbifolium*, and samples from these two phases were selected for sRNA analysis.

3.2. sRNA Profiles in the Critical Period of Sex Differentiation

To determine the tissue- or stage-specific miRNA profiles during flower development, total RNA was respectively extracted from female and male flower buds on 31 March (hereafter referred to as Fa and Ma, respectively) and 7 April (hereafter Fb and Mb, respectively) to construct four sRNA libraries, to compare the two sexes and periods during the critical sex differentiation. A total of 116,105,527 raw reads were obtained from the four libraries. After trimming the adapter sequences and filtering low-quality and short/long sequences (<15 nt or >34 nt), 109,240,787 clean reads remained for subsequent analysis. According to the Rfam database, 40.94%, 39.14%, 40.43%, and 40.21% clean reads in the Fa, Fb, Ma, and Mb libraries, respectively, were mapped to known non-coding sRNAs, including rRNAs, tRNAs, snRNAs, and other sRNAs. In addition to unknown sRNAs, the remaining 8.79%, 10.44%, 8.43%, and 10.23% clean reads, representing unique reads, were used for miRNAs identification from the Fa, Ma, Fb, and Mb library, respectively (Figure 5).

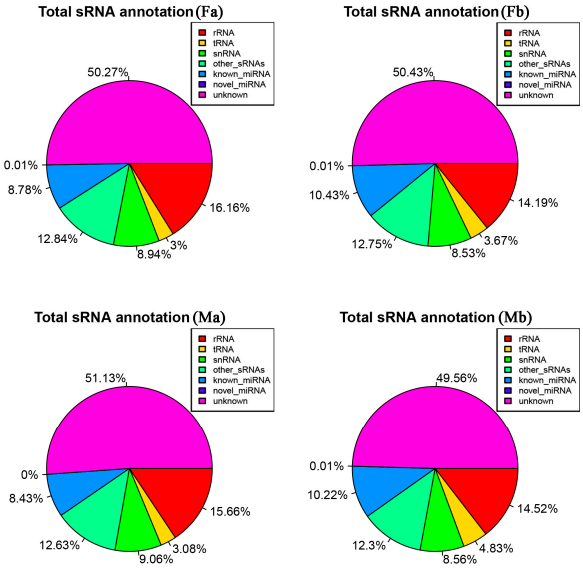

Figure 5. Classification annotation of non-coding sRNAs of *X. sorbifolium* in female and male flower buds on 31 March and 7 April. (Fa): Female flower buds on 31 March; (Ma): Male flower buds on 31 March; (Fb): Female flower buds on 7 April; (Mb): Male flower buds on 7 April.

In all libraries, examination of the sequence distributions of unique reads showed that the majority of sRNAs were 21–24 nt in length, with the majority being 24 nt, followed by 21-nt-long sRNAs (Figure 6A), which was consistent with the general size distribution of sRNA libraries reported for arabidopsis (*Arabidopsis thaliana*) [49] and rice (*Oryza sativa*) [50]. Just as miRNAs were originally found in plants [23], further analysis of conserved miRNAs revealed that the majority was 21-nt long, followed by 20-nt-long and 22-nt-long miRNAs (Figure 6B).

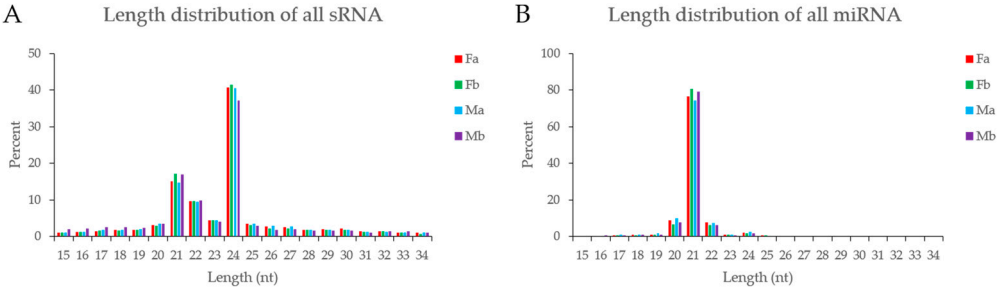

Figure 6. Length distribution of all sRNAs and miRNAs in the four libraries of *X. sorbifolium* from female and male flower buds, on 31 March (Fa and Ma, respectively) and 7 April (Fb and Mb, respectively). (**A**) Length distribution of all sRNAs; (**B**) length distribution of miRNAs.

Analysis of nucleotide bias revealed that uracil (U) was the most common nucleotide at the 5′ end, which was detected in more than 90% of the identified miRNAs and was consistent with the initial findings of miRNAs in plants [23]. The 10th nucleotide matched the cleavage site of the targets and was mainly adenine (A) or guanine (G), while the major nucleotide at another common cleavage site at the 11th nucleotide was a cytosine (C) (Figure 7).

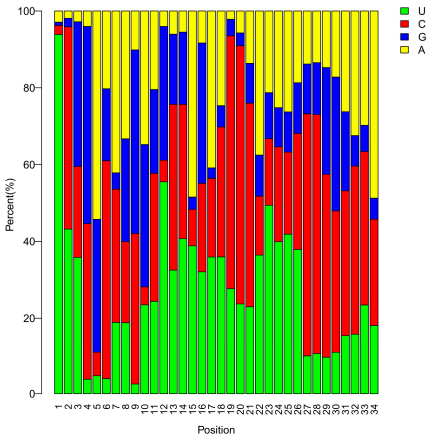

Figure 7. Relative nucleotide bias at each miRNA position compared with the total RNA of *X. sorbifolium*. U: uracil; C: cytosine; A: adenine; G: guanine.

3.3. Conserved miRNAs in the Critical Period of Sex Differentiation

The qualified sRNAs were mapped to miRbase and combined with bioinformatics prediction to confirm the mature miRNAs. A total of 1619 miRNAs in the four libraries showed high sequence similarity to known miRNAs and were thus considered to be conserved. The sequences of conserved miRNAs were listed in Table S2. The sequences were mapped to sequences of 57 other species, with the highest number of sequences mapped to gma-miRNAs of soybean (*Glycine max*) (n = 136, 8.4%), followed by mtr-miRNAs of alfalfa (*Medicago truncatula*) (131, 8.091%), bdi-miRNAs of grass (*Brachypodium distachyon*) (129, 7.968%), and osa-miRNAs of rice (*Oryza sativa*) (128, 7.906%) (Figure 8, Table S3).

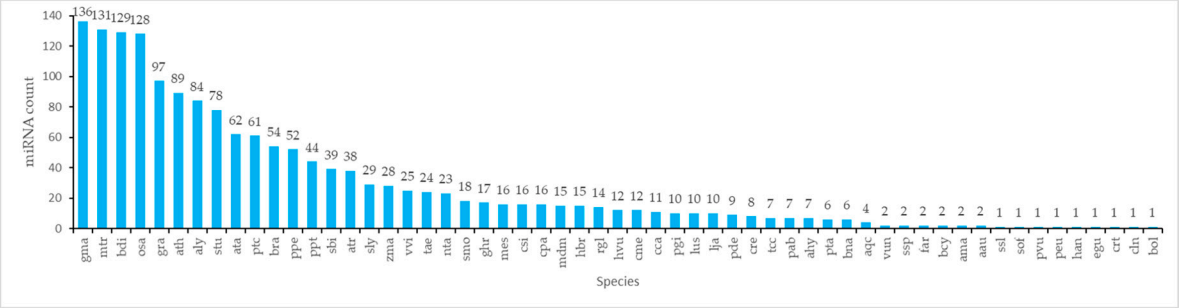

Figure 8. Species distribution of conserved miRNAs identified in *X. sorbifolium*.

The conserved miRNAs were mainly classified into 34 families (Figure 9), which are also highly conserved in other plant species. The miR156 family was the most highly represented in *X. sorbifolium* (33 members), followed by miR166 and miR171 (32 and 31 members, respectively). The number of family members of the next most dominant families, miR482, miR159, miR169, miR396, miR319, miR167, miR172, and miR395, ranged from 21 to 28. The RPM (reads per million = each miRNA read/all miRNA reads) value varied considerably among the miRNA families in Fa, Fb, Ma, and Mb libraries. In addition, the expression levels of conserved miRNAs were significantly different, even within the same family. (Table S4).

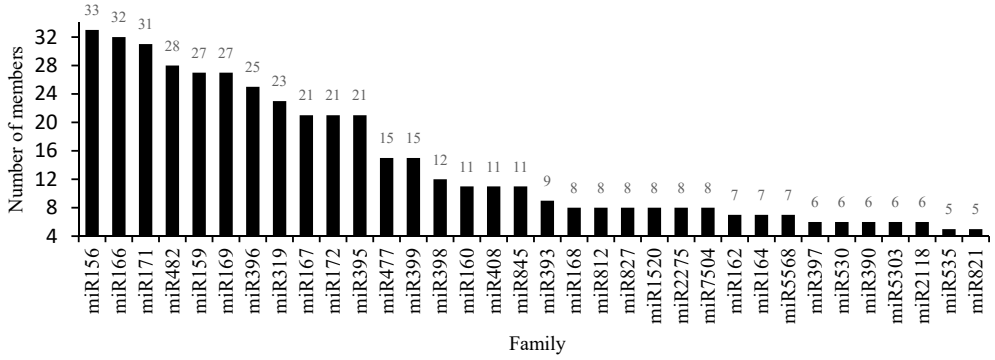

Figure 9. Distribution of the major families (with >5 members) of conserved miRNAs in *X. sorbifolium*.

3.4. Novel miRNAs in the Critical Period of Sex Differentiation

The remaining unique sRNAs that did not map to known miRNAs or other kinds of sRNAs were used to predict novel miRNAs. In total, 219 candidate miRNAs with the main size of 21 nt were considered to be novel miRNAs. The sequences of novel miRNAs and structures of pre-miRNA were all listed in Table S5. In addition, the abundance of novel miRNAs was lower than that of conserved miRNAs, which is in line with previous studies [29,51–53]. Only novel-m0271-5p and novel-m0285-5p demonstrated high RPM values (100 and 300 RPM, respectively), followed by novel-m0267-3p, novel-m0054-5p, novel-m0072-5p, and novel-m0233-5p, with RPM values over 10. The abundance of all other novel miRNAs was less than 10 RPM (Table S6). These novel species-specific miRNAs are regarded as young miRNAs that have only recently emerged in the evolutionary process.

3.5. Differentially Expressed miRNAs among the Four Libraries

To identify sex-specific miRNAs, the normalized miRNA expression levels of the four libraries were divided into four groups for pairwise comparisons: Fa vs. Fb, Ma vs. Mb, Ma vs. Fa, and Mb vs. Fb. MiRNAs with a more than 1-fold difference in expression level and adjusted p-value less than 0.05 between groups were considered to be differentially expressed between sexes or phases, which are summarized in Tables S7–S10. Overall, 162 conserved miRNAs and 14 novel miRNAs were found to

be differentially expressed in the four comparisons. The pre-miRNA structures of these differentially expressed conserved miRNAs were listed in Table S11. However, among them, only 15 conserved miRNAs and one novel miRNA expressed at high levels. In the subsequent analysis, these miRNAs were mainly discussed.

In the comparison of Fa vs. Fb, 53 miRNAs were differentially expressed, including 49 conserved and four novel miRNAs. Compared with Fa, 24 and 29 miRNAs were up- and down-regulated in Fb, respectively. Although bra-miR168a-5p_R1-16L21 was down-regulated in Fb, its expression levels in Fa (9561.212 RPM) and Fb (3673.808 RPM) were still higher than those of the other differentially expressed miRNAs identified.

In the comparison of Ma vs. Mb, 78 conserved and seven novel miRNAs were found to be significantly differentially expressed, including 40 and 45 miRNAs with up- and down-regulated expression in Mb, respectively. Some of the 45 down-regulated miRNAs were much more abundant (RPM > 10,000) in Ma than others, including ata-miR166c-3p_R1-18L21 (19,721.288 RPM in Ma) and bra-miR162-3p_R1-17L21 (11,253.918 RPM in Ma). The same applied to ata-miR396c-5p_R1-18L21 (26,288.922 RPM in Ma; 69,898.909 RPM in Mb) and ata-miR396e-5p_14T-C (57,563.624 RPM in Ma; 175,577.005 RPM in Mb) among the 40 up-regulated miRNAs. The expression levels of the miRNAs ata-miR169d-5p, cme-miR166i_R1-19L20, lus-miR159c_R1-21L21, and ppt-miR319e_R1-21L21 that were down-regulated in Mb were all higher than 1000 RPM, whereas ptc-miR6478_R1-20L21 that was up-regulated in Mb reached only 1000 RPM. Among the novel miRNAs, novel-m0271-5p showed the maximum expression level overall (194.989 RPM).

In the Ma vs. Fa comparison, 46 conserved miRNAs and two novel miRNAs were significantly differentially expressed, including 30 and 18 miRNAs that were up-regulated and down-regulated in Fa, respectively. One of these miRNAs, bra-miR168a-5p_R1-16L21, was also found to be differentially expressed in the Fa vs. Fb comparison, which was up-regulated in Fa, and showed higher expression levels than those of the other differentially expressed miRNAs in both Fa (9561.212) and Ma (3480.273). Similarly, the expression levels of pab-miR3711_R18-1L20 in Fa (1294.221) and Ma (625.401) were relatively higher than those of the other differentially expressed miRNAs. Similar to the comparison of Ma vs. Mb, novel-m0271-5p also showed a down-regulated trend in Ma.

In the Mb vs. Fb comparison, there were 23 and 22 miRNAs with up- and down-regulated expression in Fb, respectively, including 40 conserved miRNAs and five novel miRNAs. Overall, the expression levels in these two groups were low, with the highest levels detected for zma-miR2275c-5p_R21-6L21 at 689.184 and 209.510 RPM in Mb and Fb, respectively.

Comprehensive analysis of the four groups of comparisons revealed some intersections between the differentially expressed miRNAs, which are summarized in a Venn diagram in Figure 10. However, there was no miRNA at the intersection of the four comparison groups. Of the miRNAs appearing in all intersections, bra-miR168a-5p_R1-16L21 demonstrated the maximum expression level, followed by zma-miR2275c-5p_R21-6L21, nta-miR477a, cme-miR159b_R2-21L21, pab-miR396a, and novel-m0271-5p, whereas the others were expressed at relatively low levels, indicating that these highly expressed miRNAs may play crucial roles in the process of sex differentiation (Table S12).

3.6. Target Prediction and Functional Annotation

A total of 1677 putative target genes of 112 differentially expressed miRNAs (101 conserved and 11 novel miRNAs) were predicted using miRanda and RNAhybrid (Table S13). Consistent with previous studies, the same miRNA could be predicted to have multiple target genes, although the number of target genes varied considerably among the miRNAs. The miRNAs ata-miR396e-3p_R1-15L21, ata-miR396c-3p_R5-19L21, and tcc-miR399e_R1-15L21 had the highest numbers of target genes at 531, 526, and 337, respectively, whereas less than 60 target genes were predicted for the other miRNAs. This result suggested that these three miRNAs with many targets may regulate different metabolic processes and exert pleiotropic functions in flower development. Conversely, the same gene can be targeted by several miRNAs. For example, TR12296|c0_g1 was simultaneously targeted by members

of the miR156 and miR396 families, and TR1924|c0_g1 was targeted by members of the miR159 and miR319 families (Table 1).

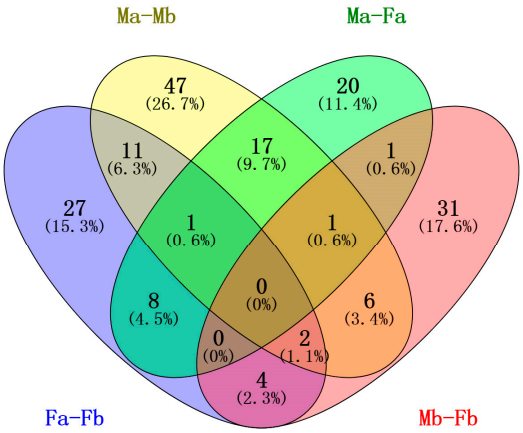

Figure 10. Venn network map of differentially expressed miRNAs in the four comparison groups of *X. sorbifolium*. (Fa) and (Ma): female and male flower buds on 31 March (before the critical sex differentiation point), respectively; (Fb) and (Mb): female and male flower buds on 7 April (at the critical sex differentiation point), respectively.

Table 1. MiRNAs and their target genes related to flower and gametophyte development of *X. sorbifolium*.

miRNA	Putative Target Gene	Target Gene Function
gma-miR393k_14G-A mes-miR393d atr-miR393	TR6435|c4_g4	Pollen maturation; Stamen development
gma-miR396e ata-miR396c-5p_R1-18L21 ata-miR396e-3p_R1-15L21	TR3538|c0_g1	Embryo sac development; Ovule development
cme-miR159b_R2-21L21 gma-miR319l gma-miR319q	TR1924|c0_g1	Flower development
cme-miR156j_R2-22L22 ata-miR156e-5p_R1-19L20_7A-G	TR12296|c0_g1	Anthers development
ata-miR156e-5p_R1-19L20_7A-G	TR10002|c0_g1 TR3055|c0_g1	Pollen tube development Flower development; Phyllotaxis development
ata-miR408-3p_R1-17L20	TR16019|c0_g1 TR10727|c0_g1	Embryo development; Flower development; Fruit development; Leaf development Organ growth
bra-miR162-3p_R1-17L21	TR9505|c0_g1	Embryo sac development
mtr-miR2673b_R17-2L22	TR1482|c0_g1	Pollen maturation
bdi-miR5169b_R7-21L21	TR4178|c0_g1	Flower development
novel-m0351-5p	TR8265|c0_g1	Anthers development
novel-m0318-5p	TR10202|c0_g1	Flower development regulation; Flower organ formation

The putative target genes of significantly differently expressed miRNAs were subjected to GO and KEGG functional annotations. GO annotation demonstrated that 697 target genes mapped to 496 functional categories representing a wide range of biological processes, cellular components, and molecular functions (Figure S1). Further analysis demonstrated that 17 miRNAs were directly

associated with flower and gametophyte development in *X. sorbifolium*, including two novel miRNAs and 15 conserved miRNAs from the miR393, miR396, miR156, miR159, miR319, miR408, miR162, miR2673, and miR5169 families (Table 1). Some miRNAs with the same target genes participated in the same biological process. For instance, members of both the miR159 and miR319 families were involved in flower development. Furthermore, a single miRNA could also participate in multiple processes, such as ata-miR156e-5p_R1-19L20_7A-G. The sequences of target genes in Table 1 were listed in Table S14.

KEGG pathway analysis showed that 82 target genes regulated by 20 of the differentially expressed miRNAs mapped to 23 metabolic pathways (Table S15), including those related to carbohydrate metabolism and glycan biosynthesis and metabolism, such as propanoate metabolism, pyruvate metabolism, starch and sucrose metabolism, fructose and mannose metabolism, glycosphingolipid biosynthesis-ganglio series, glycosaminoglycan degradation, glycosphingolipid biosynthesis-globo series, and other glycan degradation pathways. Several miRNAs from different families appeared to be involved in the same pathways (Figure S2). For example, the miR399, miR396, miR156, and miR393 families were all associated with plant hormone signal transduction. In addition, the target genes of ata-miR396e-3p_R1-15L21 mapped to most of the enriched pathways.

3.7. Validation of miRNAs

RT-qPCR was used to validate the expression levels of three novel and 16 conserved miRNAs, which were selected based on their flower-related functional annotations and higher expression levels. Similar abundance profiles were obtained by RT-qPCR analysis and high-throughput sequencing (Tables S5–S8; Figure 11). In the comparison of Fa and Fb samples, the expression levels of all miRNAs were higher in Fb, indicating their up-regulated expression during the development of female flowers. The same trend was found for the majority of miRNAs in Ma and Mb samples. These results demonstrated the credibility of high-throughput sequencing and the potential of the identified miRNAs for further in-depth analysis. Further, the credibility of the sequencing results demonstrated the reliability of the miRNAs and their functions identified in this study.

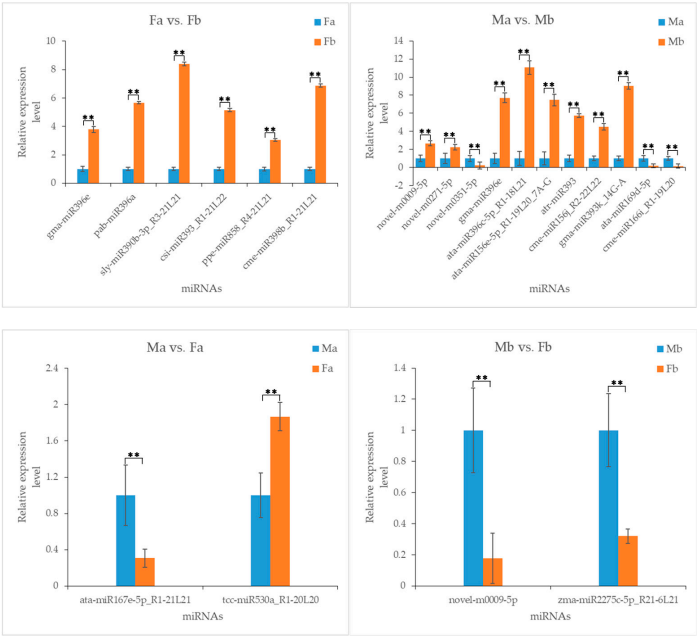

Figure 11. RT-qPCR validation of relative expression levels of miRNAs identified by high-throughput sequencing in four comparison groups. (Fa) and (Ma): female and male flower buds on 31 March (before the critical sex determination point), respectively; (Fb) and (Mb): female and male flower buds on 7 April (at the critical sex determination point), respectively; (**): p-value < 0.01, very significant differences.

4. Discussion

Previous studies have shown that sex differentiation is driven by the selective developmental arrest of the pistil and stamens [12,14]. To accurately determine the critical period of sex organ abortion, we observed pistil and stamen development across six stages in paraffin-embedded sections of *X. sorbifolium* along with external morphology of inflorescence analyses. We identified that the main structural difference between male and female flowers are characterized by distinct inflorescence elongation that generate visible separation between flower buds (7 April, 2018). As development progresses, the sex organs underwent abortion, and bisexual flowers eventually grew into unisexual flowers. The selective developmental arrest of sex organs is the most common method for generating unisexual flowers [19]. Litchi (*Litchi chinensis*) and longan (*Dimocarpus longan*), also belonging to the Sapindaceae family, show a sex differentiation process similar to that identified for *X. sorbifolium* [54–57]. In addition, fructus momordicae (*Siraitia grosvenorii*) [58] and cucumber (*Cucumis sativus*) [59], members of the Cucurbitaceae family, also undergo a "bisexual phase", followed by selective development of the sex organs or their abortion to form male or female flowers. The "bisexual to unisexual" transformation in *X. sorbifolium* suggested that various genetic mechanisms underlie unisexual flower development and that these sex-related genes will be selectively expressed.

Since the role of miRNAs in floral organ development and sex differentiation in plants is increasingly coming to light, we constructed and compared four separate sRNA libraries corresponding to different sexes at the same phase and different phases for the same sex to explore their functions during sex differentiation. Overall, we identified 1619 known miRNAs that are conserved across 57 plant species, including remarkable conservation with *Glycine max*, *Medicago truncatula*, and *Brachypodium distachyon*, suggesting a close relationship between these species and *X. sorbifolium*. These conserved miRNAs belonged to 34 miRNA families, 13 of which contained more than 15 members (miR156, miR166, miR171, miR482, miR159, miR169, miR396, miR319, miR167, miR172, miR395, miR477, and miR399). Some of these miRNA families showed high expression levels in all libraries (e.g., miR159, miR396, and miR319), confirming their broad conservation. Also, the miR396 and miR399 families had more target genes than the others, suggesting a pleiotropic role in the process of sex differentiation in *X. sorbifolium*. In addition, 219 novel miRNAs with much lower expression levels than the conserved miRNAs were identified; however, novel-m0285-5p, novel-m0271-5p, novel-m0267-3p, novel-m0054-5p, novel-m0072-5p, and novel-m0233-5p showed relatively higher expression levels, indicating their potential importance in the process of sex differentiation.

Comparisons of differentially expressed miRNAs between female and male flower buds of the same phase (Fa vs. Ma and Fb vs. Mb) and between two phases of the same sex flower bud (Fa vs. Fb and Ma vs. Mb) provided further insight into sex differentiation: if a miRNA showed significantly higher expression in Mb than in Ma and Fb, its overexpression might promote the development of male organs while preventing the maturation of female organs, and ultimately contribute to the formation of male flower; otherwise, it may play opposite roles in *X. sorbifolium* sex differentiation. Based on these comparisons, up-regulated expression of gma-miR393c-3p_R1-21L21, gma-miR4408_R16-2L24, pab-miR3709a_R15-1L21, zma-miR2275c-5p_R21-6L21, zma-miR396g-3p_R20-2L21, and novel-m0009-5p appear to promote formation of the male flower. Among these, the target genes of the miR393 family were annotated to participate in stamen development and pollen maturation, and those of the miR396 family were annotated to be associated with ovule development.

Similarly, compared to expression profiles in Fa and Mb, the up-regulation of bdi-miR169c-3p_R16-2L20, hbr-miR6174_R6-20L21, osa-miR5157b-3p_R9-24L24, and novel-m0182-5p in Fb indicated their essential functions in the formation of female flowers. A previous study also showed that miR169 regulates plant responses to abiotic stress, flower development, and flowering time by targeting transcription factors in the *NF-YA* gene family [60]. Therefore, identification of bdi-miR169c-3p_R16-2L20 in the present study may provide new insight into the function of the miR169 family. In addition, gma-miR5780d_R7-21L22 showed higher expression levels in female

flower buds than in male flower buds at every phase (Fa > Ma and Fb > Mb), also suggesting a specific role in female flower formation.

A previous study showed that overexpression of miR396 causes the stigma to bend in *Arabidopsis thaliana*, although the curved stigma does not affect the female function of the pistil [61]. In contrast to this finding, in the present study, gma-miR396e, ata-miR396c-5p_R1-18L21, and ata-miR396e-3p_R1-15L21 were all up-regulated during flower bud development in both male and female buds and were annotated to affect ovule and embryo sac development. Similarly, ata-miR408-3p_R1-17L20 was also up-regulated in both Mb and Fb, with functions related to regulation of development of the embryo and flower; however, miR408 was previously reported to be involved in response to abiotic stress [62,63]. Based on these conflicting findings, we cannot provide a definitive conclusion on the specific regulatory roles of the miR396 and miR408 families. However, our results suggest an effect on sex differentiation in *X. sorbifolium*, which warrants further investigation.

Comparisons within a group can also help to explain the functions of differentially expressed miRNAs to a certain extent. In the comparison of Ma vs. Mb, gma-miR393k_14G-A, mes-miR393d, and atr-miR393 from the miR393 family, and cme-miR156j_R2-22L22 and ata-miR156e-5p_R1-19L20_7A-G from the miR156 family were up-regulated in Mb, indicating a role in male sex differentiation. Indeed, GO functional annotation showed that the target genes of these miRNAs affect the development and maturation of the stamen, pollen, and anther. These observations were consistent with studies in *Arabidopsis*, showing that miR156 affects early anther development by targeting the SBP-box transcription factor squamosa promoter binding protein-like 8 (*SPL8*) gene [64,65]. Interestingly, miR393 has been shown to regulate flowering timing by targeting F-box auxin receptors encoded by transport inhibitor response protein 1 (*TIR1*) [66,67], although there is less evidence for its influence in the development of sexual organs in plants. Therefore, our results may extend the functions of miR393. In addition, bra-miR162-3p_R1-17L21 expression was down-regulated in Mb, with an associated function in regulating embryo sac development. However, a previous study reported that members of the miR162 family target the *DCL1* gene to negatively regulate the Dicer enzyme, and is the main factor contributing to the response to nocturnal low-temperature stress [68]. cme-miR159b_R2-21L21 from the miR159 family and gma-miR319l and gma-miR319q from the miR319 family were also down-regulated in Mb, which were annotated to regulating flower development, in line with previous studies. Members of the miR159 family can regulate the development of anthers by targeting translation initiator factors in the *MYB* family and *LFY* transcript [69–71]. The miR319 family drives multiple aspects of plant growth, including flower production, and leaf and gametophyte development by acting on *TCP* [72]. In addition to these functionally annotated miRNAs, some miRNAs with high expression levels were not annotated but may also play a crucial role in sex differentiation. For example, ata-miR166c-3p_R1-18L21, ata-miR169d-5p, cme-miR166i_R1-19L20, lus-miR159c_R1-21L21, and ppt-miR319e_R1-21L21 were significantly down-regulated in Mb, whereas ata-miR396e-5p_14T-C and ptc-miR6478_R1-20L21 were up-regulated. The extremely high expression levels of these miRNAs and their fluctuating expression during flower bud development suggest a role in male flower formation.

In the Fa vs. Fb comparison, unannotated bra-miR168a-5p_R1-16L21 showed an extremely higher expression level in Fa compared to that in Fb, indicating that it may repress the development of the female organs. Furthermore, mtr-miR2673b_R17-2L22 and bdi-miR5169b_R7-21L21, which were also down-regulated in Fb, respectively, annotated to roles in pollen maturation and flower development; however, studies on the functions of these two miRNA families are limited.

Comparing Ma and Fa, pab-miR3711_R18-1L20 was expressed at a significantly higher level than the other differentially expressed miRNAs and was up-regulated in Fa, suggesting that its overexpression may have crucial effects on female flowers formation.

In addition to the conserved miRNAs, the functions of the target genes of two novel miRNAs were also plant organ development-related. Indeed, the target gene of novel-m0351-5p regulates anther development, and that of novel-m0318-5p regulates floral organ formation and development.

5. Conclusions

In the present research, the critical period of sex differentiation of *X. sorbifolium* was determined, and four sRNA libraries from different sex flower buds of different phases were constructed to precisely illustrate the miRNAs participating in sex differentiation. The conserved and novel miRNAs were identified using high-throughput sequencing technology, and differentially expressed miRNAs were functionally annotated and further verified by RT-qPCR. Finally, multiple miRNAs were shown to be directly involved in flower and gametophyte development. Carbohydrate metabolism and glycan biosynthesis and metabolism were the primary pathways. Some miRNA functions were consistent with those reported previously, such as miR156, miR159, and miR319, while others were complemented, including miR393, miR396, miR162, miR408, miR2673, and miR5169. These results further expand our understanding of the regulatory roles of miRNAs in *X. sorbifolium* sex formation. Further research is warranted to validate the predicted functions and examine the molecular mechanisms of miRNAs identified herein. Overall, to the best of our knowledge, this is the first report regarding sex differentiation-related miRNAs in *X. sorbifolium*, and this theoretical framework can serve as a useful resource for adjusting the female–male ratio of *X. sorbifolium* and further improve the seed yield.

Supplementary Materials: The following are available online at http://www.mdpi.com/1999-4907/10/12/1141/s1, Figure S1: Go functional annotation of the target genes of differentially expressed miRNAs of *X. sorbifolium*; Figure S2: Pathway analysis of the target genes of differentially expressed miRNAs of *X. sorbifolium*; Table S1: All primer sequences involved in RT-qPCR; Table S2: The sequences of conserved miRNAs of *X. sorbifolium*; Table S3: Species and abbreviations of the conserved miRNAs of *X. sorbifolium*; Table S4: Expression (RPM) of major family members of conserved miRNAs of *X. sorbifolium*; Table S5: The sequences of novel miRNAs and structures of pre-miRNAs of X. sorbifolium; Table S6: Expression (RPM) of novel miRNAs of *X. sorbifolium*; Table S7: Differentially expressed miRNAs and their corresponding expression levels (RPM) in the group Fa vs. Fb; Table S8: Differentially expressed miRNAs and their corresponding expression levels (RPM) in the group Ma vs. Mb; Table S9: Differentially expressed miRNAs and their corresponding expression levels (RPM) in the group Ma vs. Fa; Table S10: Differentially expressed miRNAs and their corresponding expression levels (RPM) in the group Mb vs. Fb; Table S11: The structures of pre-miRNAs of differentially expressed conserved miRNAs of X. sorbifolium; Table S12: Expression levels (RPM) of miRNAs shared by multiple groups; Table S13: Number of target genes of differentially expressed miRNAs of *X. sorbifolium*; Table S14: The sequences of target genes related to flower and gametophyte development of *X. sorbifolium*; Table S15: Analysis of KEGG pathways of miRNAs and their target genes of *X. sorbifolium*.

Author Contributions: Y.A. and S.S. conceived and designed the experiments; X.W. and Y.Z. performed the experiments and analyzed the data; X.W. wrote the paper. All authors read and provided comments and approved the final manuscript.

Funding: This research was funded by the National Natural Science Foundation of China (No.31600241) and Fundamental Research Funds for the Central Universities (2015ZCQ-LX-02).

Acknowledgments: We thank the reviewers and editors for the thoughtful comments and suggestions on the manuscript. We would like to thank Yanwei Wang for participation in the design of the study. We are deeply grateful to Jinfeng Liu and Xingjie Zhang for providing materials. We also thank Editage for providing language editorial assistance.

Conflicts of Interest: The authors declare no conflict of interest.

References

1. Yu, H.Y.; Fan, S.Q.; Bi, Q.X.; Wang, S.X.; Hu, X.Y.; Chen, M.Y.; Wang, L.B. Seed morphology, oil content and fatty acid composition variability assessment in yellow horn (*Xanthoceras sorbifolium* Bunge) germplasm for optimum biodiesel production. *Ind. Crops Prod.* **2017**, *97*, 425–430. [CrossRef]
2. Qi, J.H.; Yao, Z.Y. Review on reproductive biology, propagation and breeding of *Xanthoceras sorbifolia*. *J. Northwest For. Univ.* **2012**, *27*, 91–96.
3. Li, J.; Zu, Y.G.; Fu, Y.J.; Yang, Y.C.; Li, S.M.; Li, Z.N.; Wink, M. Optimization of microwave-assisted extraction of triterpene saponins from defatted residue of yellow horn (*Xanthoceras sorbifolia* Bunge.) kernel and evaluation of its antioxidant activity. *Innov. Food Sci. Emerg. Technol.* **2010**, *11*, 637–643. [CrossRef]
4. Li, Y.J.; Xu, J.K.; Xu, P.; Song, S.; Liu, P.; Chi, T.; Ji, X.; Jin, G.; Qiu, S.; Hou, Y.; et al. *Xanthoceras sorbifolia* extracts ameliorate dendritic spine deficiency and cognitive decline via upregulation of BDNF expression in a rat model of Alzheimer's disease. *Neurosci. Lett.* **2016**, *629*, 208–214. [CrossRef] [PubMed]

5. Shao, H.B.; Chu, L.Y. Resource evaluation of typical energy plants and possible functional zone planning in China. *Biomass Bioenerg.* **2008**, *32*, 283–288. [CrossRef]
6. Shen, Z.; Zhang, K.Q.; Ao, Y.; Ma, L.Y.; Duan, J. Evaluation of biodiesel from *Xanthoceras sorbifolia* Bunge seed kernel oil from 13 areas in China. *J. For. Res.* **2019**, *30*, 869–877. [CrossRef]
7. Ao, Y. Comparison of floral ontogeny between wild-type *Xanthoceras sorbifolia* bunge and its double-flowered mutant. *Bangl. J. Bot.* **2016**, *45*, 367–375.
8. Wang, D.; Su, D.; Yu, B.; Chen, C.M.; Cheng, L.; Li, X.Z.; Xi, R.G.; Gao, H.Y.; Wang, X.B. Novel anti-tumour barringenol-like triterpenoids from the husks of *Xanthoceras sorbifolia* Bunge and their three dimensional quantitative structure activity relationships analysis. *Fitoterapia* **2017**, *116*, 51–60. [CrossRef]
9. Kong, W.B.; Liang, J.Y.; Ma, Z.X.; Zhang, J. Research advance of *Xanthoceras sorbifolia* Bunge oil. *China Oils Fats* **2011**, *36*, 67–72.
10. Harrington, K.J. Chemical and physical properties of vegetable oil esters and their effect on diesel fuel performance. *Biomass* **1986**, *9*, 1–17. [CrossRef]
11. Zhou, Q.Y.; Zheng, Y.R. Comparative de novo transcriptome analysis of fertilized ovules in *Xanthoceras sorbifolium* uncovered a pool of genes expressed specifically or preferentially in the selfed ovule that are potentially involved in late-acting self-incompatibility. *PLoS ONE* **2015**, *10*, 0140507. [CrossRef] [PubMed]
12. Ding, M.X.; Ao, Y. Research progress on the flowering and fruit set of *Xanthoceras sorbifolia* Bunge. *Chin. Agric. Sci. Bull.* **2008**, *24*, 381–384.
13. Zhou, Q.Y.; Fu, D.Z. Preliminary studies on the seproductive siology of *Xanthoceras sorbifolia*. *Sci. Silvae Sin.* **2010**, *46*, 158–164.
14. Zhang, N.; Ao, Y.; Su, S.C.; Liu, J.F.; Huang, Y.Y.; Liu, J.F.; Zhang, X.J. Analysis of morphological and anatomical features and meteorological factors during the sex differentiation in Bunge. *Acta Bot. Boreali-Occident. Sin.* **2018**, *38*, 86–97.
15. Lü, X.Q.; Zhang, M.; Wang, D.; Wang, L. Comparative study on the bisexual flower and unisexual male flower of Bunge. *Bull. Bot. Res.* **2014**, *34*, 85–94.
16. Ao, Y.; Duan, J.; Yu, H.Y.; Jiang, C.Y.; Ma, L.Y. Research progress on *Xanthoceras sorbifolia* Bunge. *J. China Agric. Univ.* **2012**, *17*, 197–203.
17. Zhou, Q.Y.; Liu, G.S. The embryology of *Xanthoceras* and its phylogenetic implications. *Plant Syst. Evol.* **2012**, *298*, 457–468. [CrossRef]
18. Hu, Q.; Gao, S.M.; Li, F.L. Pistil development in 2 types of flowers of *Xanthoceras sorbifolia*. *For. Study China* **2004**, *6*, 13–16. [CrossRef]
19. Delong, A.; Calderonurrea, A.; Dellaporta, S.L. Sex determination gene TASSELSEED2 of maize encodes a short-chain alcohol dehydrogenase required for stage-specific floral organ abortion. *Cell* **1993**, *74*, 757–768. [CrossRef]
20. Filipowicz, W.; Jaskiewicz, L.; Kolb, F.A.; Pillai, R.S. Post-transcriptional gene silencing by siRNAs and miRNAs. *Curr. Opin. Struc. Biol.* **2005**, *15*, 331–341. [CrossRef]
21. Chen, X.M. Small RNAs—secrets and surprises of the genome. *Plant J.* **2010**, *61*, 941–958. [CrossRef] [PubMed]
22. Campo, S.; Peris-Peris, C.; Siré, C.; Moreno, A.B.; Donaire, L.; Zytnicki, M.; Notredame, C.; Llave, C.; Segundo, B.S. Identification of a novel microRNA (miRNA) from rice that targets an alternatively spliced transcript of the Nramp6 (Natural resistance-associated macrophage protein 6) gene involved in pathogen resistance. *New Phytol.* **2013**, *199*, 212–227. [CrossRef] [PubMed]
23. Reinhart, B.J.; Weinstein, E.G.; Rhoades, M.W.; Bartel, B.; Bartel, D.P. Micrornas in plants. *Genes Dev.* **2002**, *16*, 1616–1626. [CrossRef] [PubMed]
24. Sun, L.X.; Pan, T.F.; Pan, D.M. Research advances on regulation of microRNAs on floral bud differentiation. *J. Anhui Agri. Sci.* **2014**, *42*, 9682–9683.
25. Zhang, Q.; Li, J.H.; Sang, Y.L.; Xing, S.Y.; Wu, Q.K.; Liu, X.J. Identification and characterization of microRNAs in Ginkgo biloba var. epiphylla Mak. *PLoS ONE* **2015**, *10*. [CrossRef] [PubMed]
26. Gupta, O.P.; Sharma, P.; Gupta, R.K.; Sharma, I. MicroRNA mediated regulation of metal toxicity in plants: Present status and future perspectives. *Plant Mol. Biol.* **2014**, *84*, 1–18. [CrossRef]
27. Allen, R.S.; Li, J.Y.; Stahle, M.I.; Dubroué, A.; Gubler, F.; Millar, A.A. Genetic analysis reveals functional redundancy and the major target genes of the *Arabidopsis* miR159 family. *Proc. Natl. Acad. Sci. USA* **2007**, *104*, 16371–16376. [CrossRef]

28. Millar, A.A.; Gubler, F. The Arabidopsis GAMYB-like genes, MYB33 and MYB65, are microRNA-regulated genes that redundantly facilitate anther development. *Plant Cell* **2005**, *17*, 705–721. [CrossRef]
29. Chen, J.L.; Zheng, Y.; Qin, L.; Wang, Y.; Chen, L.F.; He, Y.J.; Fei, Z.J.; Lu, G. Identification of miRNAs and their targets through high-throughput sequencing and degradome analysis in male and female Asparagus officinalis. *BMC Plant Biol.* **2016**, *16*, 80. [CrossRef]
30. Wu, G.; Park, M.Y.; Conway, S.; Wang, J.W.; Weigel, D.; Poethig, R.S. The sequential action of miR156 and miR172 regulates developmental timing in Arabidopsis. *Cell* **2009**, *138*, 750–759. [CrossRef]
31. Li, X.B.; Jin, F.; Jin, L.; Jackson, A.; Ma, X.; Shu, X.L.; Wu, D.X.; Jin, G.Q. Characterization and comparative profiling of the small RNA transcriptomes in two phases of flowering in Cymbidium ensifolium. *BMC Genom.* **2015**, *16*, 622. [CrossRef]
32. Banks, J.A. MicroRNA, sex determination and floral meristem determinacy in maize. *Genome Biol.* **2008**, *9*, 1–3. [CrossRef] [PubMed]
33. Le Trionnaire, G.; Twell, D. Small RNAs in angiosperm gametophytes: From epigenetics to gamete development. *Genes Dev.* **2010**, *24*, 1081–1085. [CrossRef] [PubMed]
34. Ao, Y.; Wang, Y.W.; Chen, L.; Wang, T.; Yu, H.Y.; Zhang, Z.X. Identification and comparative profiling of microRNAs in wild-type *Xanthoceras sorbifolia* and its double flower mutant. *Genes Genom.* **2012**, *34*, 561–568. [CrossRef]
35. Bi, Q.X.; Guo, B.; Zhang, D.X.; Guan, W.B. Identification and characterization of conserved and novel microRNAs in *Xanthoceras sorbifolium* via deep sequencing. *Genes Genom.* **2015**, *37*, 281–286. [CrossRef]
36. Ao, Y. Characterization and comparison of flower bud microRNAs from yellow-horn species. *Genet. Mol. Res.* **2016**, *15*. [CrossRef]
37. Martin, M. Cutadapt removes adapter sequences from high-throughput sequencing reads. *Embnet J.* **2011**, *17*, 10–12. [CrossRef]
38. Rfam. Available online: http://rfam.janelia.org/ (accessed on 21 October 2019).
39. miRBase. Available online: ftp://mirbase.org/pub/mirbase/CURRENT/ (accessed on 21 October 2019).
40. Reference genome. Available online: ftp://ftp.ensembl.org/pub/release-85/fasta/homo_sapiens/dna/Homo_sapiens.GRCh38.dna.toplevel.fa.gz (accessed on 21 October 2019).
41. Langmead, B.; Salzberg, S.L. Fast gapped-read alignment with Bowtie 2. *Nat. Methods* **2012**, *9*, 357–359. [CrossRef]
42. Meyers, B.C.; Axtell, M.J.; Bartel, B.; Bartel, D.P.; Baulcombe, D.; Bowman, J.L.; Cao, X.; Carrington, J.C.; Chen, X.; Green, P.J.; et al. Criteria for Annotation of Plant MicroRNAs. *Plant Cell* **2008**, *20*, 3186–3190. [CrossRef]
43. Enright, A.J.; Bino, J.; Ulrike, G. MicroRNA targets in Drosophila. *Genome Biol.* **2003**, *5*, 1. [CrossRef]
44. Rehmsmeier, M.; Steffen, P.; Hochsmann, M.; Giegerich, R. Fast and effective prediction of microRNA/target duplexes. *RNA* **2004**, *10*, 1507–1517. [CrossRef] [PubMed]
45. GO. Available online: http://geneontology.org/ (accessed on 21 October 2019).
46. KEGG. Available online: http://www.genome.jp/kegg (accessed on 21 October 2019).
47. Livak, K.J.; Schmittgen, T.D. Analysis of relative gene expression data using real-time quantitative PCR and the $2^{-\Delta\Delta CT}$ method. *Methods* **2001**, *25*, 402–408. [CrossRef] [PubMed]
48. Du, X.H. Study on molecular mechanism of male sterility in *Xanthoceras Sorbifolium* Bunge. Ph.D. Thesis, Beijing Forestry University, Beijing, China, 2003.
49. Rajagopalan, R.; Vaucheret, H.; Trejo, J.; Bartel, D.P. A diverse and evolutionarily fluid set of microRNAs in Arabidopsis thaliana. *Genes Dev.* **2006**, *20*, 3407–3425. [CrossRef] [PubMed]
50. Morin, R.D.; Aksay, G.; Dolgosheina, E.; Ebhardt, H.A.; Magrini, V.; Mardis, E.R.; Sahinalp, S.C.; Unrau, P.J. Comparative analysis of the small RNA transcriptomes of Pinus contorta and Oryza sativa. *Genome Res.* **2008**, *18*, 571–584. [CrossRef]
51. Mao, W.H.; Li, Z.Y.; Xia, X.J.; Li, Y.D.; Yu, J.Q. A combined approach of high-throughput sequencing and degradome analysis reveals tissue specific expression of microRNAs and their targets in cucumber. *PLoS ONE* **2012**, *7*, 33040. [CrossRef]
52. Song, C.N.; Wang, C.; Zhang, C.Q.; Korir, N.K.; Yu, H.P.; Ma, Z.Q.; Fang, J.G. Deep sequencing discovery of novel and conserved microRNAs in trifoliate orange (Citrus trifoliata). *BMC Genom.* **2010**, *11*, 431. [CrossRef]
53. Cuperus, J.T.; Fahlgren, N.; Carrington, J.C. Evolution and Functional Diversification of MIRNA Genes. *Plant Cell* **2011**, *23*, 431–442. [CrossRef]

54. Wei, Y.Z.; Dong, C.; Wang, G.; Zheng, X.W.; Li, W.C. Advances in floral bud differentiation and floral sex determination in litchi. *Guangdong Agric. Sci.* **2017**, *44*, 34–40.
55. Wang, P.; Zheng, W.; Chen, W. Fluorescence microscopic observation on flower sex differentiation in Litchi (Litchi chinensis Sonn.). *Chin. J. Trop. Crops* **2010**, *31*, 740–744.
56. Wang, H.G. Study on the cytology mechanism of flower sexual differentiation in Longan (Dimocarpus longan Lour.). Master's Thesis, Fujian Agriculture Forestry University, Fuzhou, China, 2008.
57. Wang, C.C.; Ke, G.W. An observation on the inflorescence development and the sequence of flower differentiation of Longan. *Fujian J. Agric. Sci.* **1988**, *8*, 434–436.
58. Mo, C.M.; Tu, D.P.; Huang, J. Morphological and endogenous hormones characteristics of flower bud of *siraitia grosvenorii* during its differentiation. *Acta Bot. Boreali-Occident. Sin.* **2015**, *35*, 98–106.
59. Yuan, G.F.; Zhao, Q.P.; Sun, H.Y.; Wang, Q.M. Micromorphlogical analysis of sex organ development and SDS-PAGE profile of male flowers at their later developmental stages in cucumber (Cucumis sativus L.). *J. Zhejiang Univ. Agric. Life Sci.* **2005**, *31*, 145–150.
60. Hong, Y.G.; Jackson, S. Floral induction and flower formation-the role and potential applications of miRNAs. *Plant Biotechnol. J.* **2015**, *13*, 282–292. [CrossRef] [PubMed]
61. Liu, D.M.; Yang, F.X.; Yu, D.Q. Overexpression of miR396 miRNAs caused Flower stigma curved in Arabidopsis thaliana. *Acta Bot. Yunnanica* **2009**, *31*, 353–356. [CrossRef]
62. Ma, C.; Burd, S.; Lers, A. miR408, is involved in abiotic stress responses in Arabidopsis. *Plant J.* **2015**, *84*, 169–187. [CrossRef]
63. Inês, T.; Cláudio, C.; Dalmay, T.; Fevereiro, M.P.; Santos, D.M.D. miR398 and miR408 are up-regulated in response to water deficit in Medicago truncatula. *Planta* **2010**, *231*, 705–716.
64. Xing, S.P.; Salinas, M.; Garcia-Molina, A.; Höhmann, S.; Berndtgen, R.; Huijser, P. *SPL8* and miR156-targeted *SPL* genes redundantly regulate Arabidopsis gynoecium differential patterning. *Plant J.* **2013**, *75*, 566–577. [CrossRef]
65. Xing, S.P.; Salinas, M.; Höhmann, S.; Berndtgen, R.; Huijser, P. miR156-targeted and nontargeted SBP-box transcription factors act in concert to secure male fertility in Arabidopsis. *Plant Cell* **2010**, *22*, 3935–3950. [CrossRef]
66. Chen, Z.H.; Bao, M.L.; Sun, Y.Z.; Yang, Y.J.; Xu, X.H.; Wang, J.H.; Han, N.; Bian, H.W.; Zhu, M.Y. Regulation of auxin response by miR393-targetedtransport inhibitor response protein1is involved in normal development in Arabidopsis. *Plant Mol. Biol.* **2011**, *77*, 619–629. [CrossRef]
67. Iglesias, M.J.; Terrile, M.C.; Windels, D.; Lombardo, M.C.; Bartoli, C.G.; Vazquez, F.; Estelle, M.; Casalongué, C.A. MiR393 regulation of auxin signaling and redox-related components during acclimation to salinity in Arabidopsis. *PLoS ONE* **2014**, *9*, 107678. [CrossRef]
68. Wang, X.; Liu, Y.; Chen, H.Y. The effect of low night temperature on miRNA expression in mutant and wild type tomato leaf. *Acta Hortic. Sin.* **2016**, *43*, 2369–2379.
69. Alonso-Peral, M.M.; Li, J.; Li, Y.; Allen, R.S.; Schnippenkoetter, W.; Ohms, S.; White, R.G.; Millar, A.A. The microRNA159-regulated GAMYB-like genes inhibit growth and promote programmed cell death in Arabidopsis. *Plant Physiol.* **2010**, *154*, 757–771. [CrossRef] [PubMed]
70. Gocal, G.F.W.; Sheldon, C.C.; Gubler, F.; Moritz, T.; Bagnall, D.J.; MacMillan, C.P.; Li, S.F.; Parish, R.W.; Dennis, E.S.; Weigel, D.; et al. GAMYB-like genes, flowering, and gibberellin signaling in Arabidopsis. *Plant Physiol.* **2001**, *127*, 1682–1693. [CrossRef] [PubMed]
71. Achard, P.; Herr, A.; Baulcombe, D.C.; Harberd, N.P. Modulation of floral development by a gibberellin-regulated microRNA. *Development* **2004**, *131*, 3357–3365. [CrossRef] [PubMed]
72. Schommer, C.; Bresso, E.G.; Spinelli, S.V.; Palatnik, J.F. Role of MicroRNA miR319 in plant development. *Signal. Commun. Plants* **2012**, *15*, 29–47.